



## Geotechnical characteristics of Belfast's estuarine clayey silt (sleech)

Title	Geotechnical characteristics of Belfast's estuarine clayey silt (sleech)
Author(s)	McCabe, Bryan A.;Lehane, Barry M.
Publication Date	2025-03-10
Publisher	AIMS Press
Repository DOI	<a href="https://doi.org/10.3934/geosci.2025006">https://doi.org/10.3934/geosci.2025006</a>



*Research article*

## Geotechnical characteristics of Belfast's estuarine clayey silt (sleech)

Bryan A McCabe<sup>1,\*</sup> and Barry M Lehane<sup>2</sup>

<sup>1</sup> School of Engineering, University of Galway, Galway, Ireland

<sup>2</sup> School of Engineering, University of Western Australia, Perth, Australia

\* **Correspondence:** Email: [bryan.mccabe@universityofgalway.ie](mailto:bryan.mccabe@universityofgalway.ie); Tel: +353-(0)91-492021.

**Abstract:** Belfast, the capital city of Northern Ireland and the second largest city on the island of Ireland, has experienced significant construction activity in recent years, yet relatively little has been published on the problematic soft estuarine deposits known locally as *sleech* which underlie the city and its hinterland. Results of a detailed characterization of the *sleech* at a site near Holywood, Co. Down, 8 km northeast of the city centre, are presented in this paper. This characterization was carried out in conjunction with a unique suite of full-scale foundation load tests at the site, commencing in the late 1990s. *In situ* tests clearly identified distinct sandy and silty horizons within the deposit, the bulk of which is a high-plasticity lightly-overconsolidated organic clayey silt, with clay content increasing with depth and clay fraction dominated by illite and chlorite. Both the moderate organic content and presence of diatom microfossils explain the relatively high Atterberg limits, the high compression index and the high friction angle of this material. Undrained shear strengths in triaxial compression fall at the upper end of the expected range based on a widely-used correlation with overconsolidation ratio, but are broadly compatible with *in situ* shear vane strengths corrected for plasticity index. The constant volume friction angle is remarkably insensitive to the specimen's stress history and the particle size distribution. Despite the high silt content, permeabilities and coefficients of consolidation are more typical of a clay than a silt. While the *sleech* behaviour is shown to be broadly similar to the estuarine deposits at the well-characterised geotechnical test bed at Bothkennar in Scotland, the paper illustrates that low OCR clays can have their own distinguishing characteristics.

**Keywords:** estuarine silt; *sleech*; organic; diatom microfossils; compressibility; shear strength

---

## 1. Introduction

Belfast, with a population of approximately 650,000, is the capital city of Northern Ireland (NI) and the second largest city on the island of Ireland. After the signing of the Good Friday Agreement in 1998, marking the end of a period of ethno-nationalist conflict known as “the Troubles” dating from the 1960s, the city has experienced an upsurge in construction activity. High profile examples include the Titanic Quarter, one of Europe’s largest mixed-use waterfront developments (ongoing since 2005), Victoria Square retail/leisure complex (2008), Belfast Waterfront conference/entertainment venue (renovated 2016), the new Ulster University Belfast campus (2020) and Belfast Grand Central Station (2024). Belfast’s tallest (16-storey) office building (part of the City Quays development) required continuous flight auger (CFA) piles up to 34 m long, believed to be the longest in the country [1]. The Belfast Agenda, published in 2017 and updated in 2024, is the city’s first community-led plan setting out a vision for the future of the city, including greater investment in and regeneration of the city centre.

Belfast and its hinterland are underlain by a soft grey estuarine clayey silt known colloquially as *sleech* which renders geotechnical engineering challenging, with piled foundations typically necessary for city centre buildings. An example of *sleech* clinging to a CFA auger at a Belfast site (the grey material) is shown in Figure 1. Important early contributions to our understanding of the geotechnical behaviour of the *sleech* were made at Queens University Belfast (QUB) [2–6] based on laboratory tests on block and piston samples from selected sites in the city. The interpretation of these tests was informed by research on similar soils at the time, most notably in Norway, Sweden and Canada.

Starting in the late 1990s, a programme of full-scale foundation load testing was conducted by Trinity College Dublin (TCD) at a site immediately south of Kinnegar Wastewater Treatment Works, near Holywood, Co. Down (Figure 2; coordinates near centre of site: 54.632218° N, 5.852749° W), adjacent to one of the sites previously studied by QUB in the 1970s. Both University College Dublin (UCD) and University of Galway (UG) subsequently carried out reduced-scale pile testing at the site, and laboratory-scale Push-In Resistance Tests (PIRT) in cement-stabilised *sleech* from the site were performed at UG. The key theses, journal and conference publications arising from the research are summarized in Table 1. A detailed geotechnical characterization for this site is presented in this paper, most of which is extracted from the McCabe (2002) PhD thesis [7], based on the following:

- 100 mm diameter piston samples (carried out by the NI Department of the Environment) and “Geonor” 54 mm diameter samples (carried out by TCD);
- Trial pits conducted by TCD (in material that could not be sampled);
- Classification testing including X-Ray Diffraction and Scanning Electron Microscope Analyses (TCD);
- Chemical testing (University of Massachusetts, Amherst, USA);
- Standard cone penetration tests (CPT), piezocone tests (CPTu), piezocone dissipation tests and *in situ* shear vane tests (TCD);
- Seismic cone and cone pressuremeter tests (Building Research Establishment, UK);
- Soil parameter determinations from oedometer, shear box, triaxial and ring shear tests (TCD).

The motivation for the collation and interpretation of these data herein is two-fold: (i) to assist with further interpretation of the unique set of TCD/UCD experiments and potential future testing, thereby enabling advancement of foundation engineering in soft estuarine deposits, and (ii) to provide a resource for geotechnical practitioners who encounter these challenging deposits. The data presented

are placed are context of previous QUB investigations of the *sleech*, the well-characterized Bothkennar clay-silt in Scotland [8] and other relevant literature.

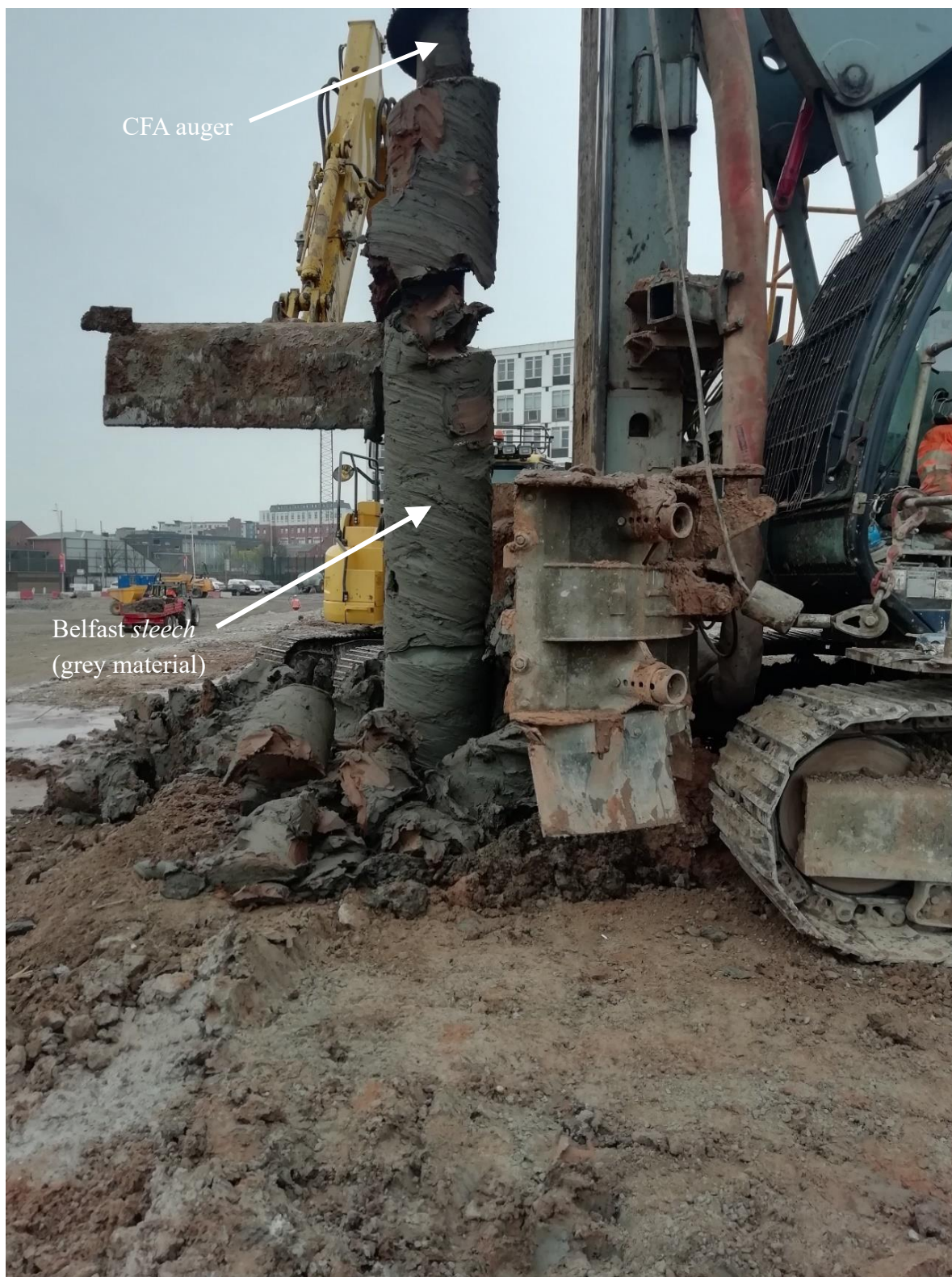


**Figure 1.** *Sleech* adhering to a CFA auger (photo courtesy of FK Lowry, Belfast).

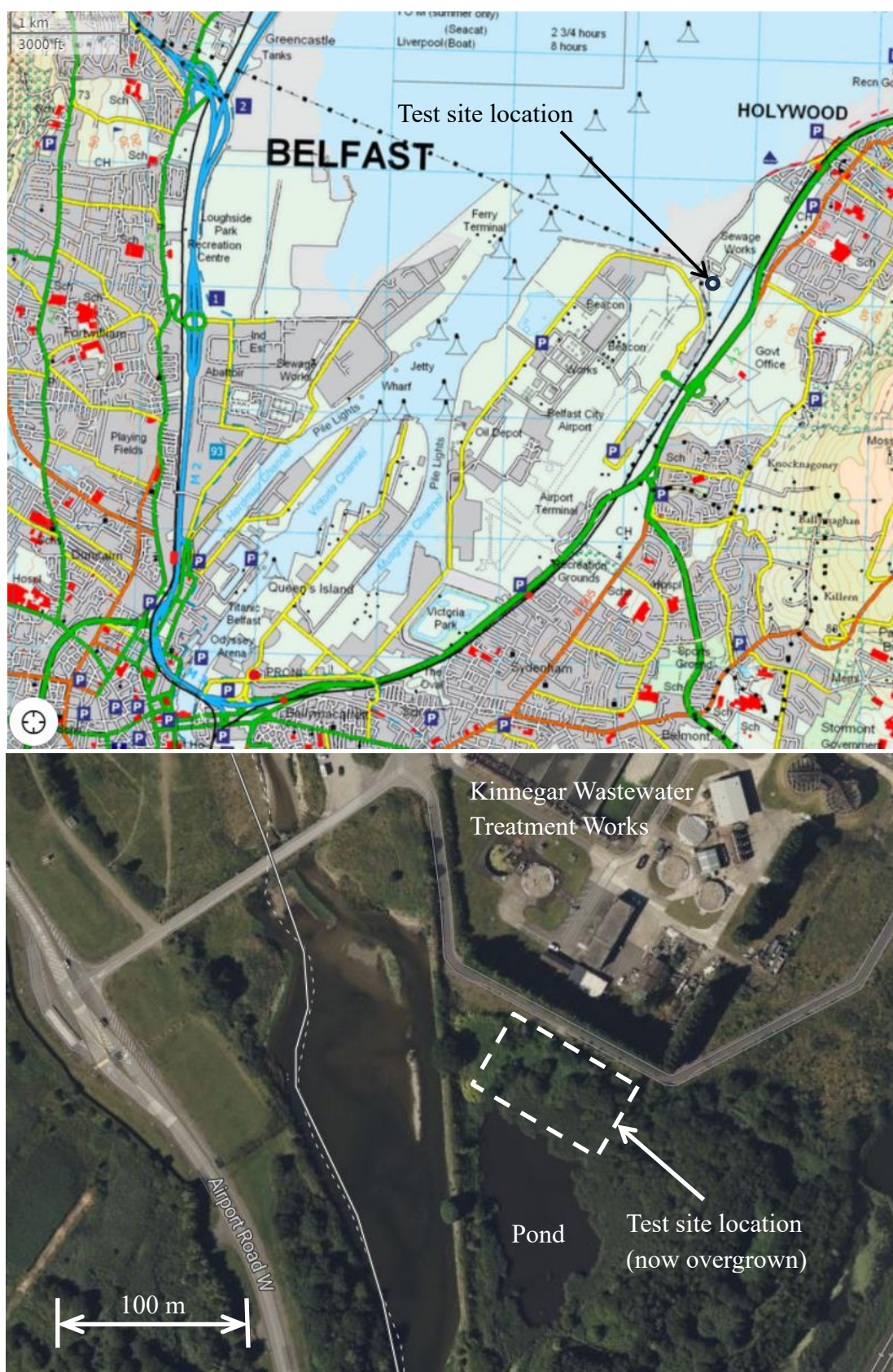


**Figure 2.** Location of Kinnegar test site (Ordnance Survey of Ireland, Google Maps).

**Table 1.** List of foundation research carried out at Kinnegar by TCD, UCD and UG.

Research topic	Theses and journal publications
Axial pile load tests: single and group	McCabe [7], Lehane <i>et al.</i> [9], McCabe and Lehane [10,11,12,13], McCabe and Phillips [14], McCabe <i>et al.</i> [15], Doherty [16], Gavin <i>et al.</i> [17], Doherty and Gavin [18], McCabe <i>et al.</i> [19]
Laterally loaded pile tests	Lehane <i>et al.</i> [20], Phillips [21]
Pad footing load test	Lehane [22]
PIRT laboratory trials	Timoney [23], Timoney and McCabe [24]

## 2. Drift Geology of the Belfast Area

The last glaciation in Ireland, known as the Midlandean, ended approximately 11,700 years ago. The Midlandean correlates chronologically with the Devensian stage in Great Britain and the Weichselian stage in northwest Europe [25]. The following summary is based on a chronology of the post-glacial geology of Belfast [5,6] informed by earlier studies [26,27].

### 2.1. Glacial deposits

The main feature of the last glacial retreat in NI was deposition rather than erosion. An extensive amount of boulder clay was formed in much of the Belfast area, with the exception of the central district and some zones in the north and east. This glacial deposit has been categorized into three distinct regions: (i) Upper Boulder Clay, which varies from a reddish-brown highly-fissured plastic clay to a stiff brown fissured stony clay, (ii) Malone Sands; well-sorted stratified and reddish-brown in colour, derived from Triassic rocks and (iii) Lower Boulder Clay, a very stiff brown silty clay with cobbles and boulders. Dark brown silty laminated clays have been found at the base of the Malone Sands and elsewhere in the Lower Boulder Clay. Both the Malone Sands and the laminations are believed to have been formed in a glacial lake during glacial retreat. Some red marine clay was also found, possibly the result of the (geologically) sudden inundation of a large area of land by the sea.

### 2.2. Post-glacial peat

An extensive deposit of peat formed immediately after glaciation in the Belfast area has been dated to be 8,000-9,000 years old (early Boreal period) by radio-carbon testing. However, this peat deposit is intermittent and appears to be absent at the Kinnegar site.

### 2.3. Estuarine deposits

The glacial retreat was followed by considerable isostatic uplift but also by a general rise in sea level [4]. While the net level of the land has risen considerably (i.e. relative to sea level) between late glacial times and the present day, there has been considerable fluctuation in the intervening period. In late Boreal times, a general rise in sea level (Flandrian Transgression) took place, covering the aforementioned peat deposits. From the late Boreal into the Atlantic period, estuarine clays were

deposited on top of the peat, primarily by the Lagan, Connswater and Blackstaff rivers, all of which confluence into Belfast Lough.

There is evidence that the estuarine deposit was formed in three phases. The Lower Estuarine clay was deposited under flat tidal conditions. Warm, low-salinity open water 5.5 m deep facilitated the deposition of the Intermediate Estuarine clay. Finally, the Upper Estuarine Clays were deposited in cooler conditions and in 9 m of salt water. This entire process took place over 3,000 years, in a depositional environment thought to have been somewhat more energetic than that of the Bothkennar clay-silt [28] with which the Belfast *sleech* is often compared. The overall thickness of estuarine deposits is believed not to exceed 15 m in the Belfast area [3]. Although grain-size, structure and organic content are highly location-dependent, the mineralogy is quite consistent throughout [2].

#### 2.4. Post-Depositional processes

Post-depositional processes influencing soil properties are believed to include bonding, leaching, fluctuations in water levels and addition of fill material [5].

### 3. Site Stratigraphy and Soil Composition

The boreholes, trial pits and cone penetration tests performed at the Kinnegar site (Figure 2) informed the summary stratigraphy in Table 2. Classification data including natural water contents and Atterberg limits, bulk unit weights and particle sizes are presented in Figure 3 (natural water contents with Atterberg limits determined in conjunction are shown as solid points, whereas hollow points represent isolated measurements). Most of the data in this figure relate to the estuarine deposits from Strata 2 and 3 between 1.0 m and 8.5/9.0 m. While these two strata are collectively referred to as *sleech*, their properties are somewhat distinct.

**Table 2.** Summary classification of Kinnegar stratigraphy.

Stratum	Depth range (m)	Soil description
1	0–1.0	Building rubble matrix with loose to dense silty SAND to very silty GRAVEL overlain by 100 mm of topsoil.
2	1.0–1.3/2.5	Loose dark grey organic very silty SAND with some clayey silt lenses and shell fragments
3	1.3/2.5–8.5/9.0	Soft dark grey organic clayey SILT with shell fragments
4	8.5/9.0–11.0	Medium dense brown silty fine to medium SAND

#### 3.1. Stratum 1

Stratum 1 is typically  $\approx 1$  m thick but reduces in thickness towards the pond south of the working area of the site (Figure 2). It is highly variable in composition. While it can generally be classified as sandy gravel or gravelly sand, topsoil was observed to extend to a depth of 1 m in certain places. Poorly-compacted building rubble, including bricks and concrete, was found at most locations. A discontinuous 100 mm thick vein of fibrous peat was found at the base of this layer in one trial pit.

### 3.2. Stratum 2 (Sandy sleetch)

Although also dark grey and containing a similar quantity of organic matter to the bulk of the deposit (i.e. Stratum 3), this stratum contains a much higher percentage of coarse silt and fine sand and is generally non-plastic. The natural water content is typically 20–45% (Figure 3). Observations made from the CPT/CPTu profiles (Section 4.1) indicate that the material classifies as a sand, a silty sand or sandy silt, with clayey silt occasionally present in trial pits. The soil contains occasional shell fragments, usually no greater than 5 mm in size, although a large flat shell (60 mm across) was found in a bulk sample from a trial pit.

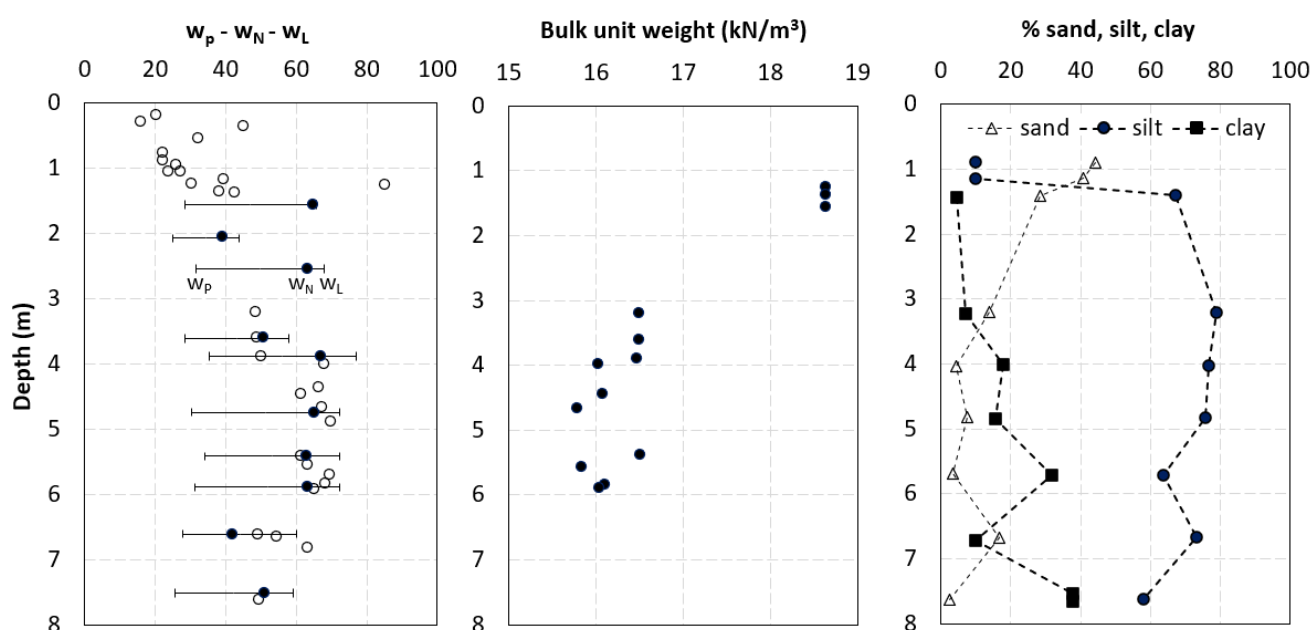


**Figure 3.** Water contents and Atterberg limits, bulk unit weights and particle sizes ( $w_p$  = plastic limit,  $w_n$  = natural water content,  $w_l$  = liquid limit).

### 3.3. Stratum 3 (Silty sleetch)

Stratum 3 comprises the bulk of the *sleetch* deposit, and its properties are summarized hereunder in terms of its clay composition and mechanical properties. A summary of Stratum 3 properties relevant to this and subsequent sections (at a reference vertical effective stress  $\sigma'_v$  of 50 kPa, corresponding approximately to mid depth of 5.5 m) is provided in Supplementary Information A.

#### 3.3.1. Clay composition

Stratum 3 may be described as an organic clayey silt, with silt content in the range 60–80%, although the clay fraction shows a general increase with depth between 8% and 38% (Figure 3). It is noteworthy that higher clay contents (typically 40–50%) are reported at an adjacent site [6]. X-Ray Diffraction analyses show that the clay fraction is principally composed of illite and chlorite. Interestingly, these are the only two clay minerals for which the measured Specific Surface Area (SSA) range of  $\approx 50$ –83  $\text{m}^2/\text{g}$



and Cation Exchange Capacity (CEC) range of  $\approx 40\text{--}43$  meq/100g can co-exist [29]. Smaller quantities of kaolinite were identified, in addition to traces of pyrite, dolomite and plagioclase feldspar. The swelling material smectite was also found in a poorly crystallized form. Chemical analyses on material smaller than  $40\ \mu\text{m}$  (i.e. between 75% and 95% of the material, mainly silt-sized) indicated a composition comprising 50% quartz, 12–21% dolomite and 4–7% calcite [30].

Scanning Electron Microscope images confirmed the presence of clay minerals and the increase in clay fraction with depth evident in Figure 3, in addition to a significant quantity of diatoms, examples of which are shown in Figure 4. Diatoms are microscopic, single-celled algae with siliceous (silicon dioxide or silica) cell walls called frustules, found in coastal or marine environments. The presence of diatoms in silts and clays can have a marked effect on their physio-chemical behaviour [31]. The organic content, determined by the loss upon ignition method at  $450^\circ\text{C}$ , was typically  $11.3 \pm 0.2\%$ . The much lower  $4 \pm 1\%$  previously quoted [4] pertains to the higher ignition temperature of  $850^\circ\text{C}$  which is no longer recommended. The pH of the *sleech* was  $\approx 8$  [23], in keeping with the pH of salt water, which is typically slightly alkaline (range 7.5 to 8.5).

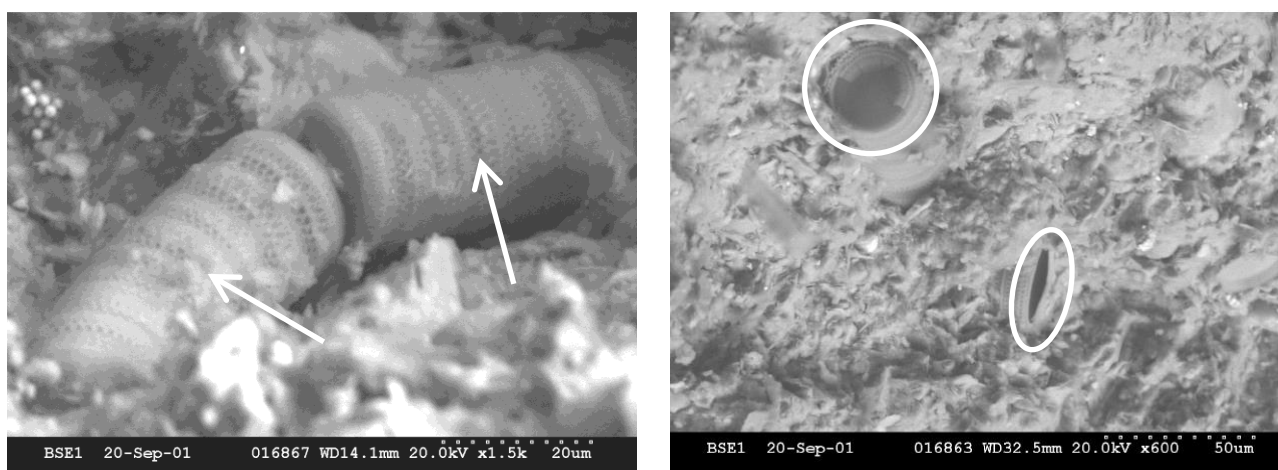


**Figure 4.** Scanning Electron Microscope images of *sleech* showing diatoms.

### 3.3.2. Mechanical Properties

While the bulk unit weight of the *sleech* ( $16.2 \pm 0.3\ \text{kN/m}^3$ ) is low for a silt or clay, this value can be justified using a weighted specific gravity based on the known proportions of mineral and organic material, adopting  $G_s = 2.73$  for the mineral component [23] and assuming  $G_s = 1.4$  for cellulose. Therefore, the hollow structure of the diatoms appears to be a secondary factor in the low bulk density. The natural water content ( $w_n$ ) within Stratum 3 is typically  $60 \pm 10\%$ , with a mean liquid limit ( $w_L$ ) of  $65 \pm 10\%$  and plasticity index ( $I_p$ ) of  $35 \pm 5\%$ . The high  $w_n$  and  $I_p$  values explain the “stickiness” of the material demonstrated in Figure 1. Adopting a reference  $\sigma'_v = 50\ \text{kPa}$ , corresponding roughly to mid-depth (5.5 m) within Stratum 3, the *sleech*'s  $I_p$  value of 38% falls below those noted in the literature for a selection of other low OCR soils (considering  $\text{OCR} < 2$  only), e.g. 45% at Onsøy, Norway [32] and in Bangkok clay [33], 48% at Bothkennar, Scotland [8] and 57% at Burswood, Australia [34].

Both Atterberg limits are higher than might be expected for a silty material. Diatoms have the effect of increasing both plastic and liquid limits, without any appreciable effect on the plasticity index [31].

The Stratum 3 *sleech* plots in the high and very high plasticity range of the Casagrande plasticity chart, on or above the A-line (Figure 5) in a zone typically associated with illites [35]. The Bothkennar clay-silt [8] plots in a similar zone, although it classifies predominantly as a very high plasticity soil. The average liquidity index of  $\approx 0.8$  is a value commonly encountered in lightly-overconsolidated materials. Activity reduces from  $\approx 4$  at the top of the layer to  $\approx 1$  at the base, higher than might be expected given the predominance of illite noted in chemical testing, but the presence of diatoms may explain the inflated activity values [31].

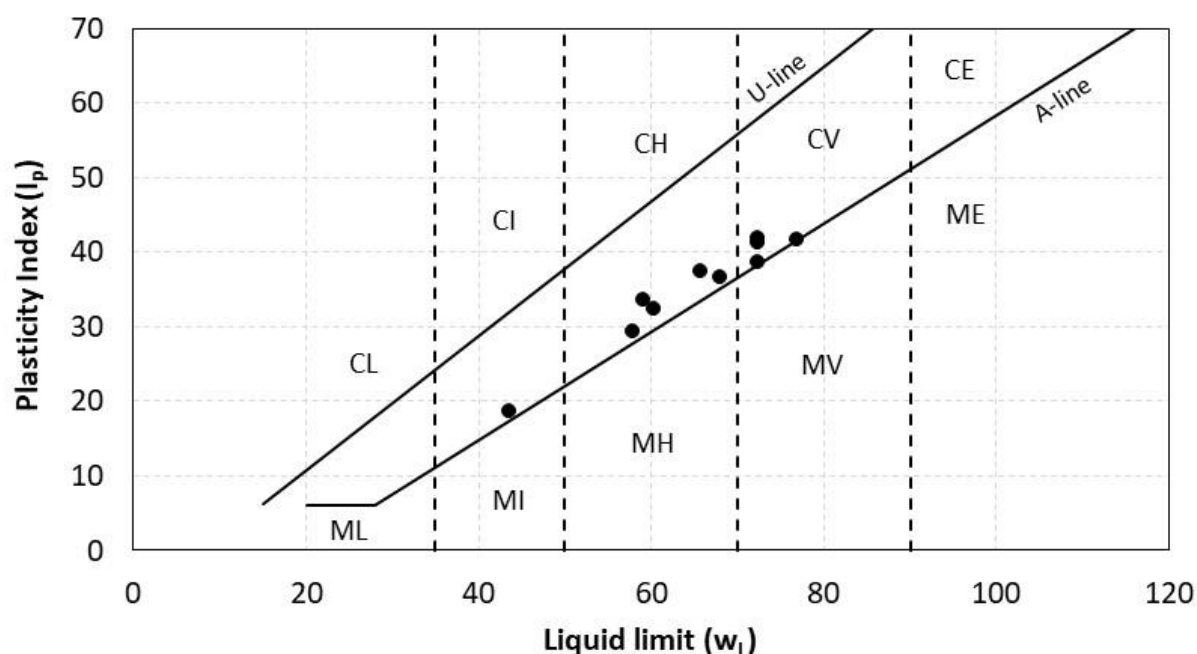


**Figure 5.** Stratum 3 *sleech* represented on Casagrande's plasticity chart.

A number of Atterberg limit determinations performed on samples with the organic fraction removed (by loss on ignition at 450°C) indicated that the liquid limit fell by  $\approx 20\%$  but the plastic limit remained unchanged (resulting in a shift to the intermediate plasticity range). This reduced plasticity, in the context of Bothkennar clay-silt [28], is likely to be more indicative of its mechanical characteristics (e.g. greater frictional strength). Sample inspections revealed that at least part of the organic fraction was composed of coarse fibrous plant material, which does not contribute to an apparent high plasticity. As with the Bothkennar clay-silt, the organic fraction is therefore also likely to comprise the residue of marine organisms which have attached themselves to the clay.

### 3.4. Stratum 4 and below

No laboratory tests were performed on Stratum 4 but from visual inspections, it is a uniform fine to medium sand. Below 11 m, boreholes conducted by the NI Dept. of the Environment indicate alternating clay and sand layers of varied thicknesses and consistencies. The maximum depth of exploration recorded in these boreholes was  $\approx 36$  m, terminated on either a boulder or basalt dyke.

#### 4. *In situ testing*

Summary results of the *in situ* testing at Kinnegar are provided in Figure 6, including the average and range of several CPT/CPTu cone tip resistance ( $q_c$ ) profiles (10 cm<sup>2</sup> Geomil cone), peak uncorrected strengths from *in situ* (cased) Geonor shear vanes ( $s_{u-vane}$ ), shear wave velocities from seismic cone testing ( $V_s$ ) and limit pressures from cone pressuremeter (CPM) testing ( $p_{LIM}$ ).

##### 4.1. *Cone penetration and piezocone testing*

The  $q_c$  data display clear transitions between Strata 1/2 and Stratum 3 in all cases. The significant variability in the consistency of the fill (Stratum 1) and the sandy *sleech* (Stratum 2) is evident. For example, the lower bound  $q_c$  profile suggests a virtual absence of Stratum 2, while the upper bound  $q_c$  profile indicates relatively competent soils with  $q_c$  as high as 7 MPa (beyond the limits plotted in Figure 6) to a depth of 2.5 m. The  $q_c$  values in Stratum 3 are much lower but remarkably uniform, despite the variations in composition indicated in Figure 2. Total cone tip resistances  $q_t$  (i.e.  $q_c$  corrected for pore pressures acting on the cone shoulder,  $u_2$ ) within Stratum 3 increase linearly with depth from  $\approx 200$  kPa at 2.5 m to  $\approx 400$  kPa at 8 m. Interestingly, the  $q_t$  value of 310 kPa at 5.5 m falls below that at Onsøy (350 kPa, [32]), Burswood ( $\approx 400$  kPa, [34]) and Bothkennar (450 kPa, [28]) at a corresponding reference  $\sigma'_v$  value of 50 kPa.

When represented on Robertson's [36] normalized cone tip resistance  $Q_t$  versus normalized pore pressure  $B_q$  chart for one of the CPTu tests (Figure 7), differences between the compositions of the three strata are apparent. Stratum 1 (Zone 6: *sands; clean sands to silty sands* and Zone 7: *gravelly sand to sand*) and Stratum 2 (Zone 5: *sandy mixtures; silty sand to sandy silt* and Zone 6 again) classify as predominantly sandy materials, whereas Stratum 3 is a clay/silt (Zone 3: *Clays; clay to silty clay* and Zone 4: *Silt mixtures; clayey silt to silty clay*).

$N_{kt}$  values were calculated by relating mean  $q_t$  values to mean  $s_{u-vane}$  values scaled by 0.85–0.9 (Bjerrum's correction for plasticity index of 35–40%) at the depths of the  $s_{u-vane}$  measurements.  $N_{kt}$  was found to vary from  $\approx 10$  at 2.5 m to  $\approx 15$  at 8 m. Piezoball factors ( $N_{ball}$ ) in the same range (i.e. 10–15) have also been reported for the *sleech* [38]; although the undrained strengths used in deriving these were based on the undrained triaxial compression tests reported in Section 6, these were comparable to the  $s_{u-vane}$  values.

Although CPTu pore pressure measurements ( $u_2$ ) were not always reliable, probably due to inadequate saturation of the porous element, values increased linearly from the groundwater level to  $200 \pm 50$  kPa at the base of the *sleech* layer (note that the groundwater table varied between 1.0 m and 1.3 m below ground level, attributable to seasonal and tidal variations). Piezocone dissipation tests indicated that the horizontal coefficient of consolidation,  $c_h$  (back-calculated using the procedure of Houlsby and Teh [39]) fell in the range 7–12 m<sup>2</sup>/year. Interestingly,  $c_h$  values in the range 100–1000 m<sup>2</sup>/year (early in the dissipation process) reducing to 20–30 m<sup>2</sup>/year (late in the dissipation process) were back-calculated from piezometer records made during and after the installation of a small pile group at the Kinnegar site [19]. These much larger  $c_h$  values are probably ascribable to macro scale effects.

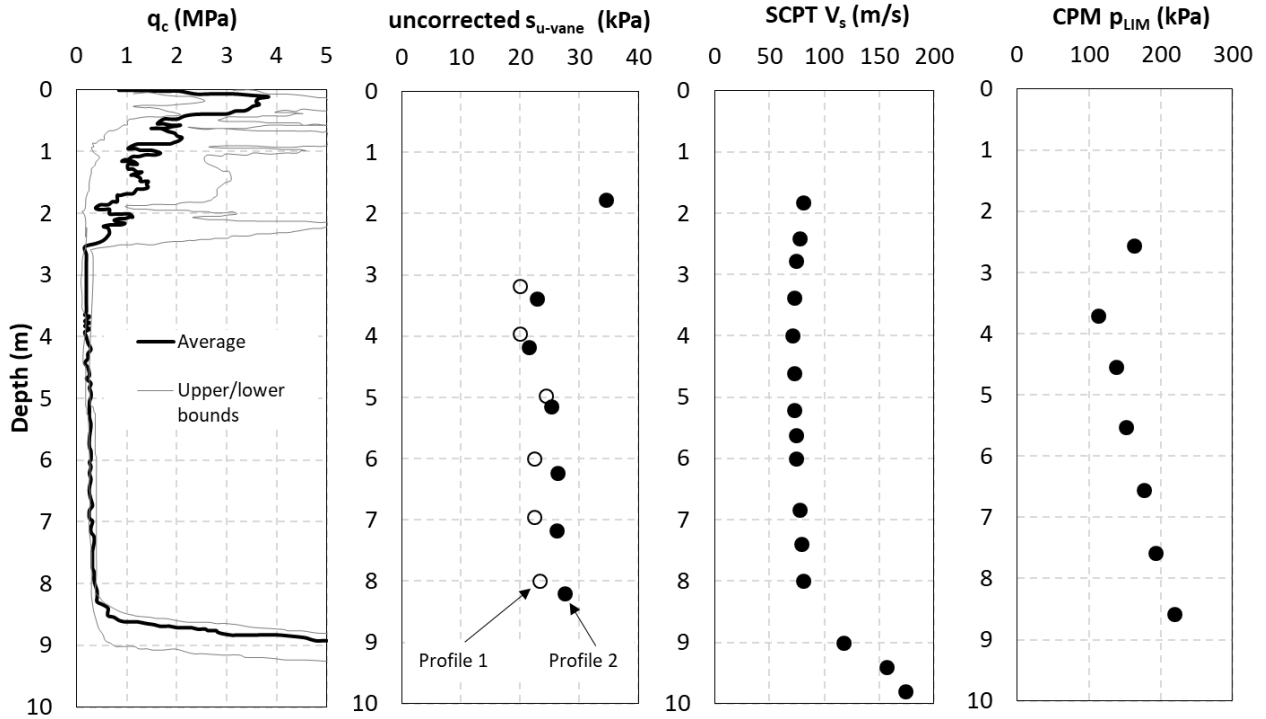


Figure 6. Summary of *in situ* testing at Kinnegar.

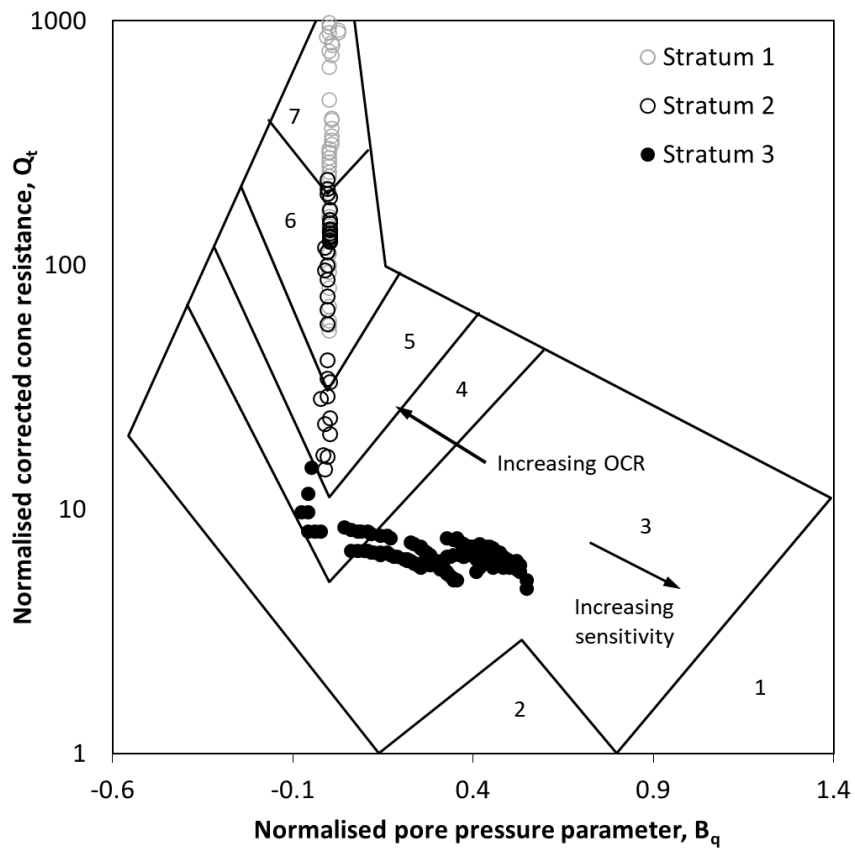


Figure 7. Robertson's (1990)  $Q_t$ - $B_q$  chart, distinguishing between Strata 1, 2 and 3.

## 4.2. Other *in situ* testing

The stronger consistency of Stratum 2, compared to Stratum 3, is confirmed by the higher *in situ* shear vane strength ( $s_{u\text{-vane}} = 35$  kPa) and (slightly higher) shear wave velocities, both measured at 1.9 m, and the higher CPM  $p_L$  value at 2.3 m. Within Stratum 3, uncorrected  $s_{u\text{-vane}}$  values increase marginally over the corresponding depth interval from  $\approx 20$  kPa to  $\approx 25$  kPa,  $V_s$  values increase marginally from  $\approx 72$  m/s to  $\approx 80$  m/s, while  $p_{LIM}$  values almost double from  $\approx 110$  kPa to  $\approx 220$  kPa. In addition to the  $q_t$  values discussed in Section 4.1, the other *in situ* measurements in Figure 6 ( $s_{u\text{-vane}}$ ,  $V_s$  and  $p_{LIM}$ ) also fall below those reported for Bothkennar clay/silt [8]. The percentage reduction in  $s_{u\text{-vane}}$  when large rotational displacements were applied in the *in situ* shear vane test, a reflection of sensitivity, is similar at both sites (35–50%). The small strain shear modulus ( $G_{seis}$ ) was estimated from the shear wave velocities according to  $G_{seis} = \rho V_s^2$ , where  $\rho$  is the bulk density of the *sleech* presented in Figure 3. This resulted in  $G_{seis}$  values in the range 8.5–10.5 GPa for Stratum 3.

## 5. 1-D Compression

A number of incremental load oedometer tests (with a load increment ratio of one) were performed on *sleech* from Stratum 3; the initial  $\sigma'_v$  was typically 6.25 kPa and specimens were loaded to at least 400 kPa, followed by three unload steps. Selected void ratio ( $e$ ) versus  $\log \sigma'_v$  plots are provided in Supplementary Information B. Profiles of preconsolidation pressure ( $\sigma'_{vy}$ ), yield stress ratio (YSR =  $\sigma'_{vy}/\sigma'_v$ ; equivalent to overconsolidation ratio OCR for 1-D compression), compression ( $C_c$ ) and swelling ( $C_s$ ) indices inferred from these tests are presented in Figure 8 and discussed hereunder.

### 5.1 Overconsolidation

Values of preconsolidation pressure ( $\sigma'_{vy}$ ), derived using Casagrande's construction, were found to be relatively constant with depth at  $50 \pm 10$  kPa. Vertical yield stress ratios (YSR) varied from  $\approx 1.6$  at a depth of 3.2 m to about unity below 6 m. This light overconsolidation is in keeping with the liquidity index of  $\approx 0.8$  noted in Section 3.3. The YSR values are slightly lower than those previously reported at Kinnegar [4], probably due to the addition of the fill layer (i.e. Stratum 1) in the meantime; the pre-filling YSR profile [4] is virtually coincident with that reported at Bothkennar [40]. Water table fluctuations and long-term creep settlements have been deemed the principal sources of the observed light overconsolidation in the deposit [4]. Constant differences between yield stress and vertical effective stress when plotted against depth typically reflect groundwater fluctuations at some stage in a deposit's geological history. This has been shown to hold true for block samples of Belfast *sleech* [4], although the effect of sampling disturbance may have concealed this trend in the most recent tests.

### 5.2 Compressibility

The compression index ( $C_c$ ) of the intact soil was found to be relatively independent of vertical effective stresses up to 1 MPa (unlike at Bothkennar) and varied between 0.4 and 0.67, averaging 0.56. The presence of diatoms is known to increase compressibility [41]. This may be reflected in the fact that the correlation between  $C_c$  and the natural water content for Irish soft soils [42] in equation (1) produces

underpredictions averaging  $\approx 15\%$  for these data (note that five of the 61 entries in the database underpinning the correlation are from the Kinnegar site). Compression indices derived from an oedometer specimen reconstituted at a water content of  $1.3w_L$  (i.e.  $C_c^*$ ) were in close agreement with those deduced from the correlation between  $C_c^*$  and  $e_L$ , the void ratio at  $w_L$  ([43], equation 2). Use of this correlation for all oedometer tests indicated a relatively constant  $C_c/C_c^*$  ratio of  $1.3 \pm 0.1$ . Swelling indices ( $C_s$ ) are typically 4–6 times lower than  $C_c$  values but also correlate well with the liquid limit.

$$C_c = 0.014(w_n - 22.7) \quad (1)$$

$$C_c^* = 0.256(e_L - 0.04) \quad (2)$$

The *sleech* showed a tendency to creep in the oedometer tests and the creep coefficient ( $C_\alpha$ ) was determined from the slope of the strain versus log time plot over a period of seven days after the end of primary consolidation (identified using Casagrande's root time method). The variation of  $C_\alpha$  with vertical effective stress is shown in Figure 9a; values were generally below 0.025 in the overconsolidated range and between 0.015 and 0.04 in the normally consolidated (NC) range. The ratio of  $C_\alpha/C_c$  was typically 0.04–0.05 for the upper part of the deposit and a little lower at greater depths. This range is at lower end of what might be expected for an organic clay or silt [44] but similar to  $C_\alpha/C_c$  of 0.03–0.05 quoted for Bothkennar [8].

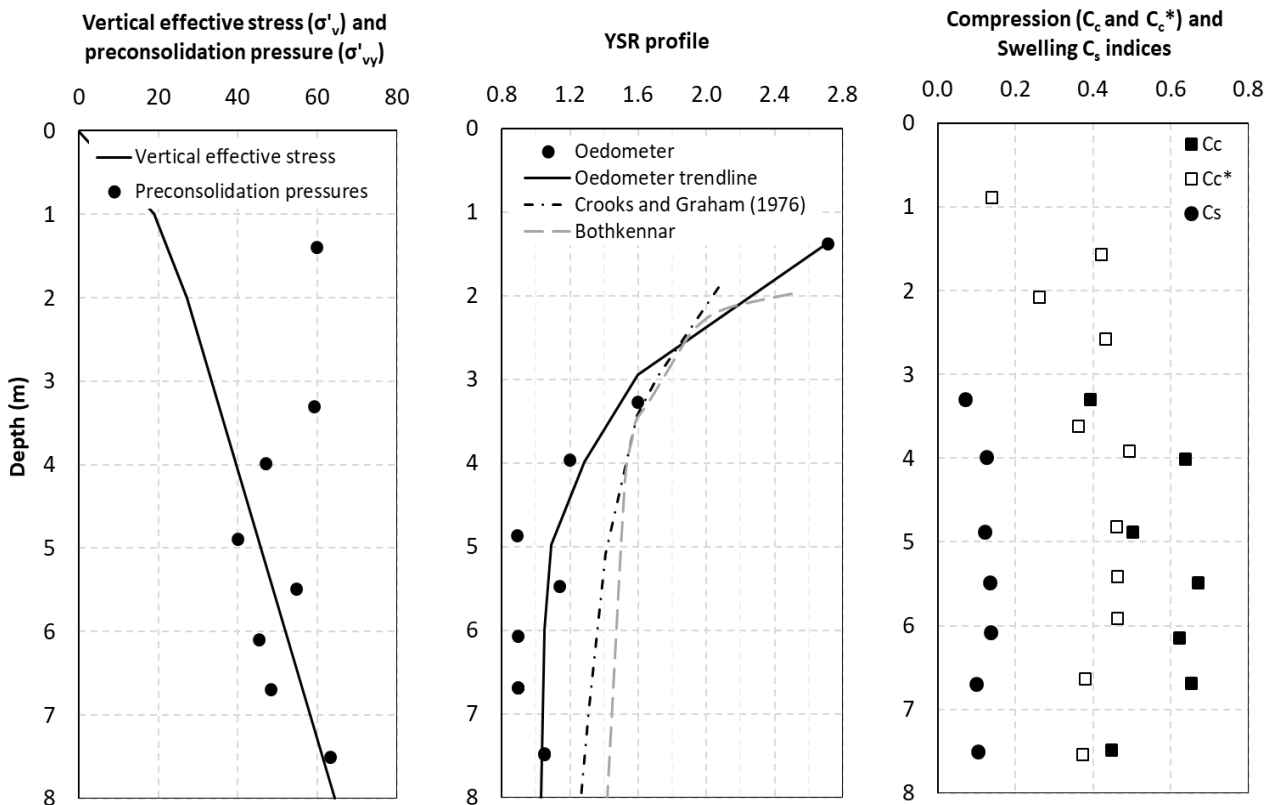


**Figure 8.** Results from oedometer tests (preconsolidation pressure and YSR profiles, compression and swelling indices).

### 5.3 Permeability and Coefficient of Consolidation

The vertical permeability estimated from oedometer tests on the material in Stratum 3 reduced with increasing stress levels (Figure 9b) but was typically in the range  $1 \times 10^{-10}$  to  $3 \times 10^{-10}$  m/s at *in situ* stress levels. As part of a ground investigation for the construction of a shallow tunnel within the *sleech* at nearby Sydenham in the 1970s, similar low vertical permeabilities were reported [45]. These permeabilities fall significantly below those reported at other low OCR sites (again benchmarked at  $\sigma'_v = 50$  kPa):  $9 \times 10^{-10}$  m/s at Onsøy [32],  $\approx 1 \times 10^{-9}$  m/s in Boston Blue Clay [46],  $1.5 \times 10^{-9}$  m/s at Bothkennar [8] and  $3.3 \times 10^{-9}$  m/s at Burswood ([47]; generic value, depth not specified), and interestingly, do not appear to be consistent with a significant presence of diatoms [31]. Vertical coefficients of consolidation ( $c_v$ ) derived from the same set of tests (Figure 9c) ranged from 0.2 to 2.8 m<sup>2</sup>/year (averaging  $\approx 1$  m<sup>2</sup>/year) at *in situ* stress levels, significantly smaller than the piezocone-derived  $c_h$  values, as is typically the case. Despite the high silt content in Stratum 3, it appears that the clay fraction is sufficiently influential for the soil mass to have permeabilities and coefficients of consolidation more typical of a clay than a silt.

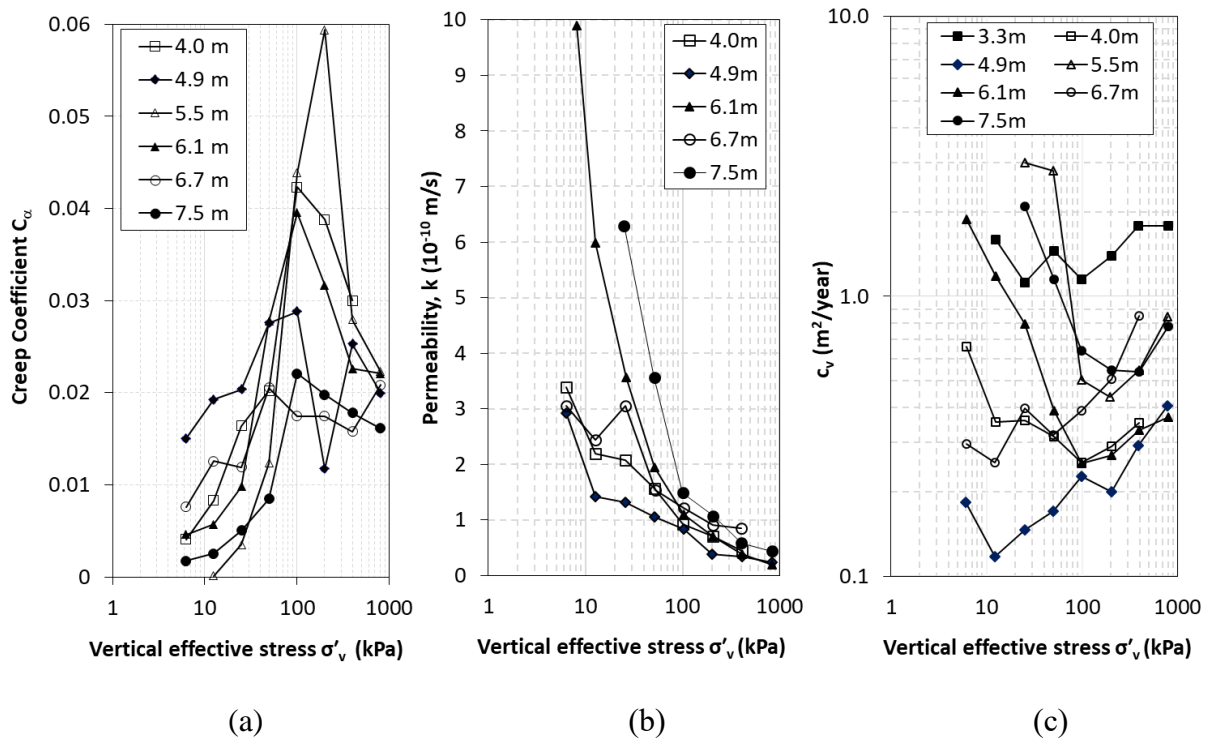


**Figure 9.** Variation of (a) creep coefficient, (b) permeability and (c) coefficient of consolidation with vertical effective stress.

By way of comparison, oedometer  $c_v$  values for *sleech* in the range  $\approx 1$ –14 m<sup>2</sup>/year and under  $\approx 1$  m<sup>2</sup>/year at vertical effective stresses below and above 100 kPa respectively were reported at Dock St. in the city in the 1980s [48]. Interestingly, their  $c_v$  against vertical effective stress relationships, back-calculated from pneumatic piezometer data under a trial embankment, exceeded oedometer values at stresses below the preconsolidation pressure, but corresponded well in the NC range.

## 6. Shear Strength

### 6.1. Stress paths

A series of ten isotropically-consolidated undrained (CIU) and anisotropically-consolidated undrained (CAU) tests were performed on 38 mm, 54 mm (Geonor) and 100 mm diameter samples from Stratum 3. The *in situ* stress was recovered approximately (or other stress states established) by consolidation and swelling to artificially induce the required level of overconsolidation. In the CAU tests, a coefficient of earth pressure at rest ( $K_0$ ) of 0.5 was used for anisotropic consolidation, approximating  $K_0$  calculated from Jaky's [49] empirical equation with friction angle for normally consolidated soils. A slightly larger value ( $K_0 = 0.6$ ) was used for anisotropic swelling to capture the light overconsolidation imposed. The 54 mm diameter subset was afforded a one-day "ageing" period. In all tests, undrained shearing was conducted at an axial strain rate of 4.5% per day. The sensitivity of *sleech* to sample disturbance has previously been highlighted [6], which manifested in some of the samples as (i) a tendency for dilation at mobilized friction angles of  $\approx 30^\circ$ , and (ii) axial strains required to develop peak deviator stresses (typically  $\varepsilon_a > 5\%$ ) were much higher than might be obtained had superior sampling techniques, such as Sherbrooke or block samples, been available ( $\varepsilon_a \approx 0.1\text{--}1\%$ ).

Stress paths (in  $q$ - $p'$  space) are shown for a set of four 38 mm CIU compression tests (CIUC) which were subjected to different levels of imposed isotropic overconsolidation (Figure 10). The stress paths corresponding to OCR values of 1, 1.5 and 2 are typical of lightly-overconsolidated soils, with contraction reflected in the sharp drop in deviator stress as the mean effective stress falls and the mobilized friction angle increases. On the other hand, the stress path for the specimen with OCR = 4.9 shows a dilatant response consistent with a more heavily overconsolidated state. Corresponding stress paths for two 54 mm CAU compression tests (CAUC) are shown in Figure 11, again exhibiting post-peak contractant behaviour. The sharper peak of the two was reached at a much lower  $\varepsilon_a$  value ( $\approx 0.5\%$ ).

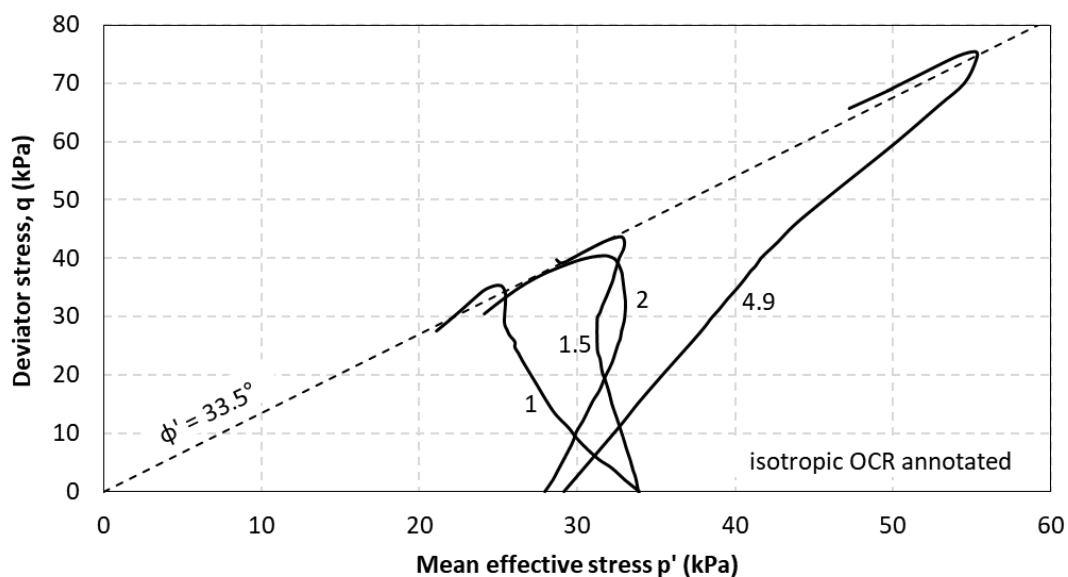


**Figure 10.** Stress paths for 38 mm CIU compression tests at various OCR values.



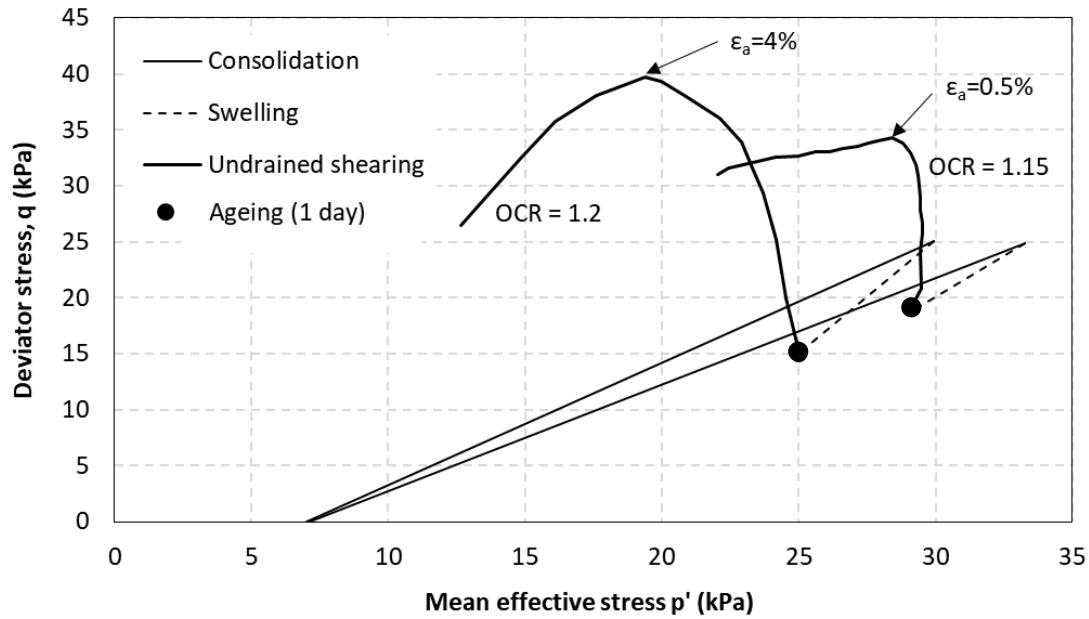


**Figure 11.** Stress paths for 54 mm CAU compression tests.

## 6.2. Undrained strength in triaxial compression and extension

Measured values of the undrained strength ratio determined in the triaxial compression tests ( $s_{utc}/\sigma'_v$ ) are compared in Figure 12 with the range proposed in equation (3) [50]:

$$\frac{s_u}{\sigma'_v} = \left( \frac{s_u}{\sigma'_v} \right)_{NC} OCR^{0.8} = (0.3 \pm 0.05) OCR^{0.8} \quad (3)$$

where the subscript “NC” refers to the normally consolidated state. Some of the measured undrained stress ratios, primarily from the anisotropic tests, appear to be somewhat higher than anticipated, but nevertheless are in keeping with values from earlier QUB studies [4]. Two CAUC tests which exhibited dilation are noted on Figure 12.

Laboratory values of  $s_{utc}$  are typically in the range 18–25 kPa and show no clear trend with depth (Figure 13), due to the counteracting effect of increasing overburden pressure and reducing YSR with depth. Corresponding  $s_{utc}/\sigma'_v$  values are similar to Bothkennar values [8]. If an average yield stress of  $\sigma'_{vy} = 50$  kPa is adopted, the ratio  $s_{utc}/\sigma'_{vy}$  is typically 0.36–0.5. Superior quality samples are likely to have yielded both higher individual  $s_{utc}$  and  $\sigma'_{vy}$  values and higher  $s_{utc}/\sigma'_{vy}$  ratios. Nevertheless, these  $s_{utc}$  values agree reasonably well with the Bjerrum-corrected  $s_{u-vane}$  results (Figure 13); such conformity between field and laboratory undrained strengths was also evident at Bothkennar. The results of two triaxial extension tests (one CIUE and one CAUE) are also included in Figures 12 and 13. Values of  $s_{ute}$  are typically 13–15 kPa and thus are lower than  $s_{utc}$  values; with corresponding  $s_{ute}/\sigma'_v$  therefore also lower than  $s_{utc}/\sigma'_v$ . Values of  $s_{ute}/\sigma'_v$  are again in keeping with those for Bothkennar clay [8].

The dependence of the undrained strength of normally consolidated *sleech* on axial strain rate was investigated in two CIUC tests on 54 mm diameter samples from Stratum 3. These were isotropically consolidated to a mean effective stress ( $p'_i$ ) of 100 kPa and subjected to triaxial compression, at a lower

axial strain rate initially, followed by a faster axial strain rate. These tests indicate that  $s_u/p'_i$  ratios increase by a factor of  $\approx 15\%$  for each log cycle increase in strain rate, over a range of 0.001%/min to 1 %/min. Strain rate determinations on triaxial specimens by QUB [4] indicated rate effects in the range 8–17% per log cycle, with much of the data in the 10–12% range (for a plasticity index of  $\approx 40\%$ ).

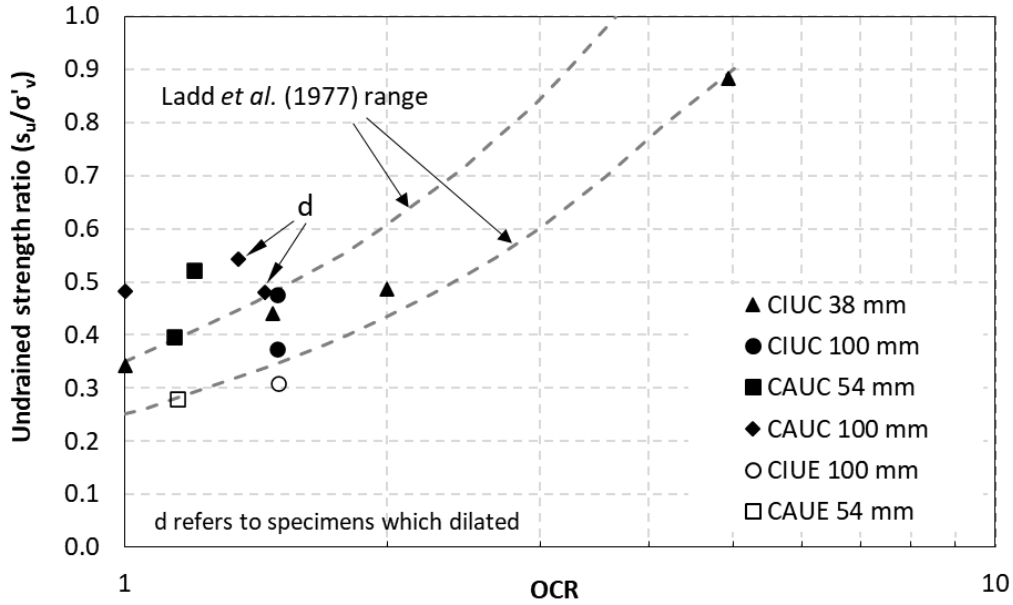


Figure 12. Undrained strength ratios from CIU, CAU tests as a function of OCR.

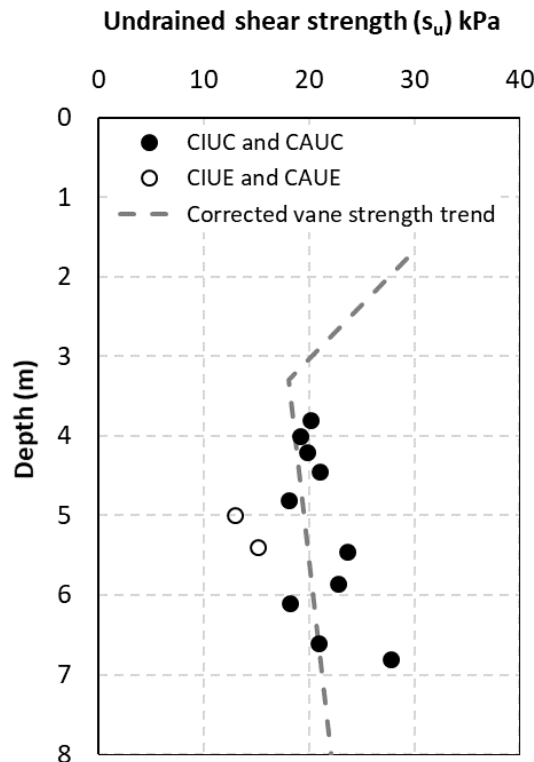
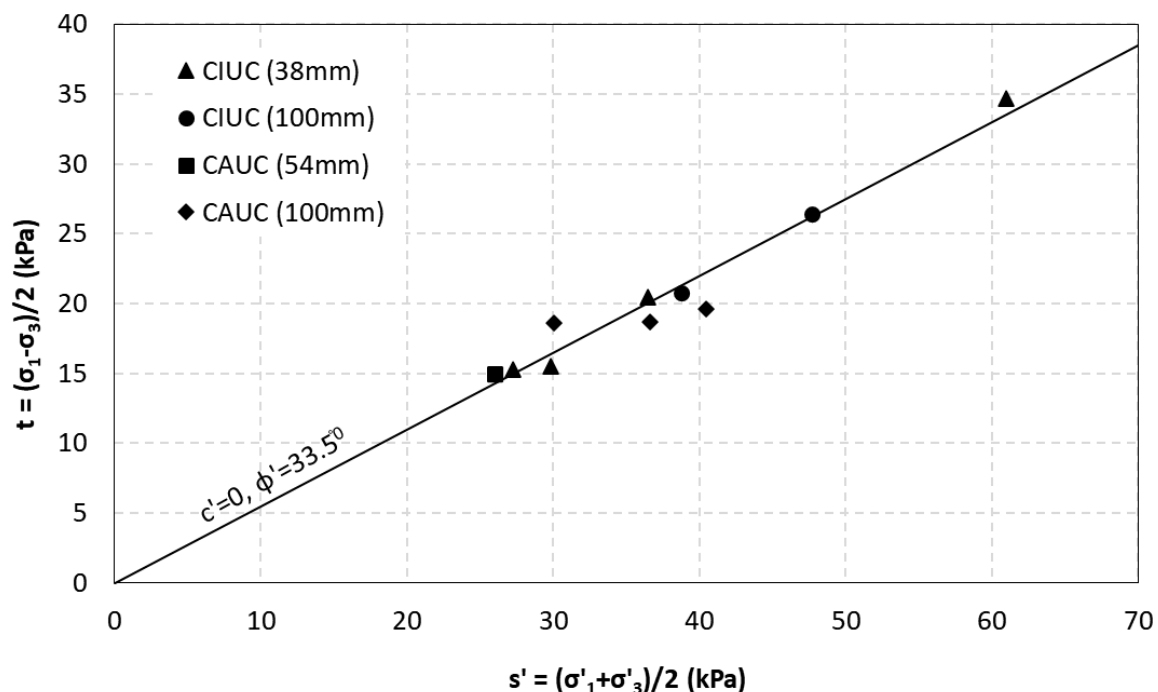


Figure 13. Undrained strength profile from CIU and CAU triaxial tests and shear vane.

### 6.3. Effective stress strength in triaxial compression and direct shear

Effective stress strength parameters for *sleech* from Stratum 3 were derived from the consolidated undrained triaxial tests and shear box tests reconsolidated to normal effective stresses between 50 kPa and 200 kPa. The values of stress invariants  $t$  and  $s'$  at ultimate conditions ( $\approx 10$ – $20$  % axial strain) are plotted in Figure 14 for the CIUC and CAUC tests. The ultimate shear strength is represented very well by a cohesion intercept  $c' = 0$  and constant volume friction angle  $\phi'_{cv} = 33.5^\circ$ , with  $\phi'_{cv}$  showing low sensitivity to the specimen's stress history, particle size distribution and sample quality. This relatively high friction angle is comparable to that of the Bothkennar clay-silt ( $34^\circ$ ), which has a slightly higher clay fraction but lower percentage of clay minerals, which is more in keeping with the plasticity index of the material when the organics are removed [51]. Moreover, the presence of diatoms can increase the angle of internal friction of a host soil, due to the rough surfaces of the frustules and their propensity for interlocking [41].

Shear box tests carried out on 60 mm reconstituted specimens at 0.0244 mm/min revealed the contractant behaviour typical of lightly overconsolidated materials, with the absence of a peak shear stress. Plots of ultimate friction angle (calculated assuming  $c' = 0$ ) are plotted against normal effective stress in Figure 15 for *sleech* in Strata 2 and 3. The values of  $\phi'_{cv}$  in Stratum 3 vary from  $34^\circ$  at a vertical effective stress  $\sigma'_v = 50$  kPa to  $26^\circ$  at  $\sigma'_v = 200$  kPa; the former stress level is most representative of the *in situ* stress state, which shows good agreement with  $\phi'_{cv}$  derived from the CIUC and CAUC tests in Figure 14. The slightly higher  $\phi'_{cv}$  values in Stratum 2 reflect its lower water content and coarser composition relative to Stratum 3.



**Figure 14.** Stress invariants ( $t$  versus  $s'$ ) plot for triaxial compression data (intact samples), ( $\sigma'_1$  = major principal effective stress,  $\sigma'_3$  = major principal effective stress).

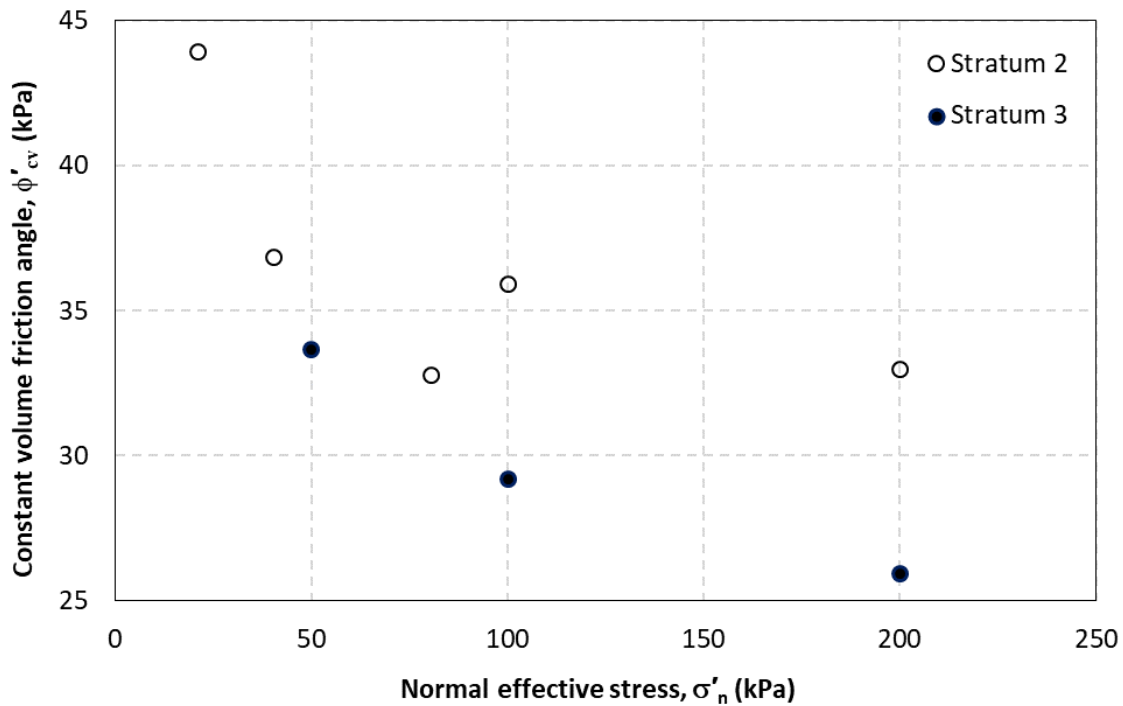


**Figure 15.** Shear stress versus normal effective stress from shear box tests (reconstituted samples).

### 6.3. Residual strength

Although not true interface tests, soil-on-soil ring shear tests were conducted in a Bromhead apparatus following recommendations for ring shear testing aimed at displacement pile design [52], which was the primary focus of the Kinnegar research. After consolidation to a normal effective stress of 100 kPa, specimens were first subjected to a large displacement at the fast (undrained) shearing rate of 4.5 mm/min to model pile installation. Samples were then sheared at a slow drained rate of displacement of 0.035 mm/min. The difference between peak ( $\phi'_{p,res}$ ) and residual ( $\phi'_{res}$ ) angles was typically no greater than  $1^\circ$ . Values of  $\phi'_{res}$  are plotted with depth in Figure 16, with the aforementioned individual  $\phi'_{cv}$  values from triaxial and shear box tests shown for reference. Despite the sparsity of data at depths shallower than  $\approx 3$  m, it is clear that  $\phi'_{res}$  falls only slightly below  $\phi'_{cv}$  measured in triaxial compression and that the shearing mode is “turbulent” in this region [53]. However, below this depth, the difference is more significant;  $\phi'_{res}$  reduces which depth from  $25.5^\circ$  at  $\approx 4$  m to  $22.5^\circ$  at  $\approx 7$  m. This reduction with depth is in keeping with the increasing clay content, with the magnitudes indicating a “transitional” sliding mode, i.e. where both turbulent and sliding shear arise in different parts of the shear zone [53].

A number of *sleech* specimens were subjected to ring shear tests against an interface. Peak interface friction angles of  $\approx 16^\circ$  were measured for a rough concrete interface, with post-peak softening resulting in a reduction of  $1^\circ$  to the residual interface friction angle [54]. Corresponding peak and residual interface friction angles based on a smooth stainless steel interface were  $11^\circ$  and  $10^\circ$  respectively [55]. In the latter interface test set, the authors reported a similar rate effect (14% per log cycle) in the range  $\approx 0.1$  mm/sec and  $\approx 30$  mm/sec to that observed in the CIU tests.

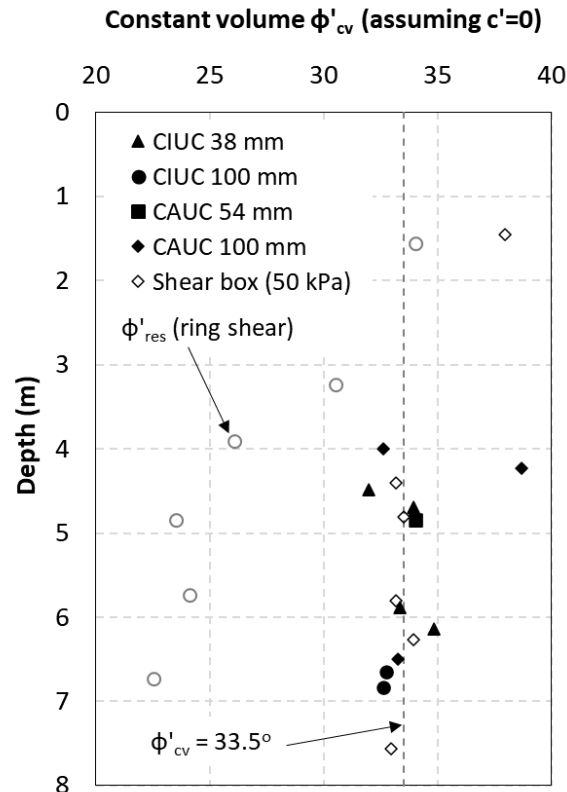


**Figure 16.** Variation of residual friction angle with depth, in context of constant volume friction angle from triaxial and shear box tests.

## 7. Shear Stiffness

Local strain measurements were made on the triaxial compression and extension specimens using Hall effect transducers. Typical small strain secant shear stiffness values  $G_{sec}$  (calculated from Young's modulus  $E_{sec}$  with Poisson's ratio  $\nu=0.5$  for undrained conditions), normalized by the initial mean effective stress at the beginning of undrained shearing  $p'_0$  ( $\approx 29$  kPa in this case) are shown in Figure 17.  $G_{sec}/p'_0$  values for the *sleech* are generally slightly lower than those measured for the Bothkennar clay-silt, also shown in the figure. Values of  $G_{sec}/p'_0$  (compression) extrapolated back to 0.001% strain are  $\approx 50\%$  higher than  $G_{seis}/p'_0$  (with  $p'_0 \approx 29$  kPa) values in the range 300–360 derived from shear wave velocities (Section 4.2).

## 8. Conclusions

The *sleech* found extensively under Belfast and its environs is a soft organic lightly-overconsolidated estuarine clayey silt. Key learnings specific to the Kinnegar site shown in Figure 2 are as follows:

- Beneath a fill layer, the profile comprises a sandy horizon with a maximum thickness of  $\approx 1.5$  m, underlain by a silty horizon in excess of 6.0 m thick constituting the bulk of the deposit. These horizons are clearly distinguished by *in situ* testing. Within the silty horizon, the corrected cone tip resistance is lower than that documented for other lightly-overconsolidated soils.

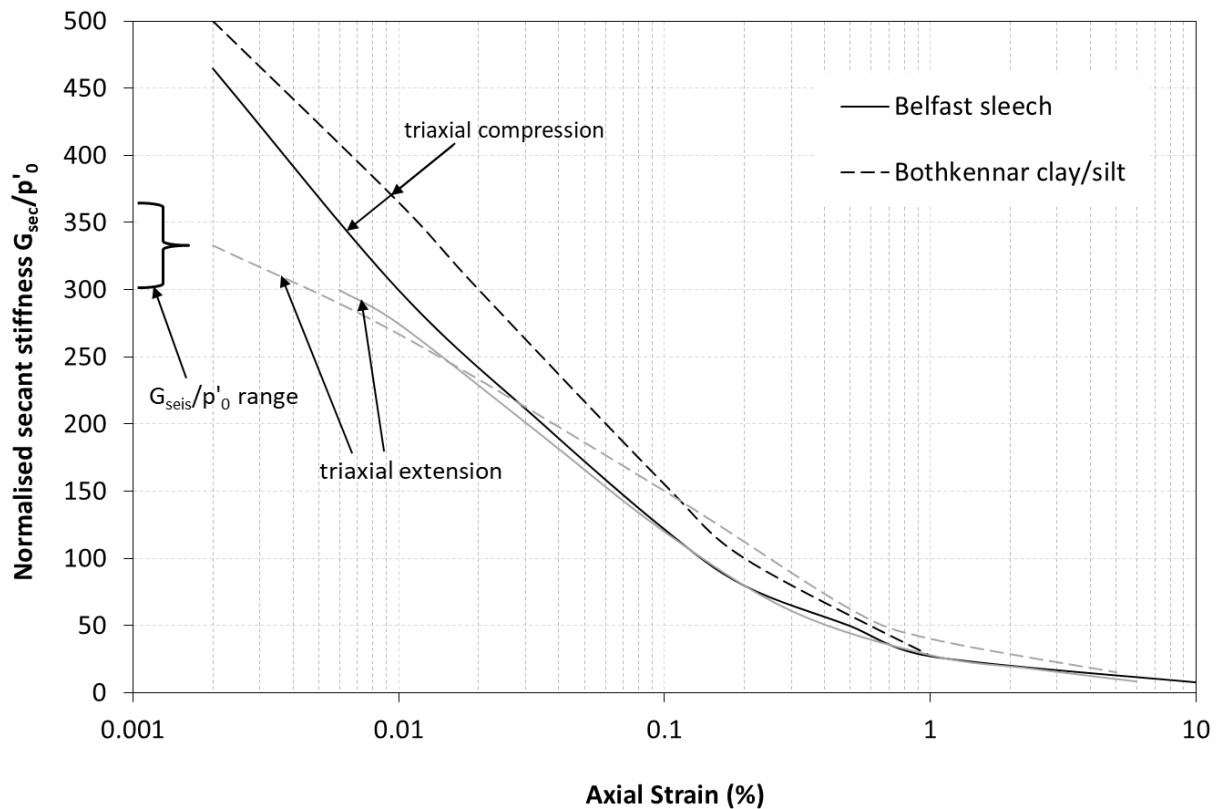


**Figure 17.** Secant shear stiffness normalized by mean effective stress against axial strain ( $p'_0 = 29$  kPa).

- Despite having in excess of 60% silt content throughout the bulk of the deposit, liquid limit and plasticity index data plot above the A-line indicative of an inorganic clay of high or very high plasticity. However, this interpretation is complicated by the presence of diatom microfossils which inflate both consistency limits (but not the plasticity index) and a moderate organic content which increases the plasticity index. The low bulk density, high compression index and high constant volume friction angle can also be explained by one or both of these factors.
- Permeabilities and coefficients of consolidation derived from oedometer testing are more consistent with expectations for a clay than a silt and are also considerably lower than those noted for a selection of low OCR clays in the literature.
- The clay fraction comprises mainly of illite and chlorite. The clay fraction increases with depth, with the undrained shear strength and compression index also displaying mild increases with depth. The constant volume friction angle is largely insensitive to particle size distribution and stress history, but the residual friction angle shows the expected reduction with clay content.
- Undrained strengths derived from triaxial compression tests tally reasonably well with *in situ* vane strengths corrected for plasticity index and fall at the lower end of the “soft” range, although superior quality samples are expected to yield slightly higher values. The undrained strength ratio is slightly higher than might be expected based on a well-known correlation with OCR. Secant shear modulus values at small strains normalized by initial mean effective stress significantly exceed the corresponding values derived from shear wave velocities.

The Belfast *sleech* clearly exhibits trends comparable to other lightly-overconsolidated estuarine clay-silt deposits documented in the literature, such as the Bothkennar clay-silt in Scotland. However, this paper has shown that such deposits can have their own distinctive (and sometimes unexpected) characteristics. This observation, coupled with the significant variation in the *sleech* composition and organic content across Belfast noted by several authors (including between this site and the adjacent QUB site at Kinnegar) highlights the importance of site-specific characterization for any given construction project. The particular focus of the characterization will be guided by the application, for example: (i) organic content, clay fraction mineralogy can be used to aid characterisation, (ii) sensitivity and interface friction angle to inform driven pile designs, (iii) undrained shear strength anisotropy for shallow foundation designs, and (iv) compression index, coefficients of consolidation (vertical and horizontal) and creep coefficient for road embankments projects.

### Use of AI tools declaration

An Artificial Intelligence (AI) tool was used to generate the list of recent high-profile construction projects in Belfast used within the first paragraph of the Introduction.

### Acknowledgements

The first author's PhD was funded by an Ussher Fellowship (TCD) at the time of the study. The authors would like to acknowledge the important contribution of the technical staff at TCD, in particular the late Mr. Martin Carney, to the programme of field and laboratory tests. The contribution of NI Dept. of the Environment and the Building Research Establishment (UK) to sampling and *in situ* testing respectively is also appreciated. Thanks also to Farimah Fattahi Masrour and Dr. Kevin Flynn for digitizing many of the figures.

### Conflict of interest

The authors declare no conflict of interest.

### References

1. Hancock M (2019) Ground improvement: slaying the *sleech*, Ground Engineering. Available from: <https://www.geplus.co.uk/features/ground-improvement-slaying-sleech-20-11-2019/>.
2. Crooks JHA (1973) Laboratory studies of the Belfast estuarine deposits. PhD thesis, Queens University Belfast.
3. Crooks JHA, Graham J (1972) Stress-strain properties of Belfast estuarine clay. *Eng Geol* 6: 275–288. [https://doi.org/10.1016/0013-7952\(72\)90012-9](https://doi.org/10.1016/0013-7952(72)90012-9)
4. Crooks JHA, Graham J (1976) Geotechnical properties of the Belfast estuarine deposits. *Géotechnique* 26: 293–315. <https://doi.org/10.1680/geot.1976.26.2.293>
5. Bell A (1977) Laboratory Studies of the Belfast Estuarine Deposits. PhD Thesis, Queen's University of Belfast.

6. Gregory BJ, Bell AL (1991) Geotechnical properties of Quaternary deposits in the Belfast area. *Geol Soc Eng Geol Spec Publ* 7: 219–228. <https://doi.org/10.1144/GSL.ENG.1991.007.01.20>
7. McCabe BA (2002) Experimental investigations of driven pile group behaviour in Belfast soft clay. PhD thesis, Trinity College Dublin.
8. Hight DW, Paul MA, Barras BF, et al. (2003) The characterization of Bothkennar Clay. *Charact Eng Prop Nat Soils* 1: 543–597.
9. Lehane BM, Jardine RJ, McCabe BA (2003) One-way axial cyclic tension loading of driven piles in clay. *Proceedings of the BGA International Conference on Foundations*, 493–506.
10. McCabe BA, Lehane BM (2003) Stress changes associated with driving pile groups in clayey silt. *Proceedings of the 13<sup>th</sup> European Conference on Soil Mechanics and Geotechnical Engineering*, National University of Ireland Galway, 2: 271–276.
11. McCabe BA, Lehane BM (2006) Behavior of axially loaded pile groups driven in clayey silt. *J Geotech Geoenviron Eng* 132: 401–410. [https://doi.org/10.1061/\(ASCE\)1090-0241\(2006\)132:3\(401\)](https://doi.org/10.1061/(ASCE)1090-0241(2006)132:3(401))
12. McCabe BA, Lehane BM (2006) Prediction of pile group response using a simplified non-linear finite element model, *Methods in Geotechnical Engineering*, CRC Press, Graz, 589–594.
13. McCabe BA, Lehane BM (2008) Measured and predicted t-z curves for a driven single pile in lightly overconsolidated silt. *Proceedings of the 3<sup>rd</sup> International Conference on Site Characterization*, Taipei, 487–491.
14. McCabe BA, Phillips DT (2008) Design lessons from full-scale foundation load tests. *Proceedings of the 3<sup>rd</sup> International Conference on Site Characterization*, Taipei, 615–620.
15. McCabe BA, Gavin KG, Kennelly ME (2008) Installation of a reduced-scale pile group in silt. *2<sup>nd</sup> BGA International Conference on Foundations*, IHS BRE Press, Dundee, 1: 607–616.
16. Doherty P (2010) Factors affecting the capacity of piles in clay. PhD thesis, University College Dublin.
17. Gavin KG, Gallagher D, Doherty P, et al. (2010) Field investigation of the effect of installation method on the shaft resistance of piles in clay. *Can Geotech J* 47: 730–741. <https://doi.org/10.1139/T09-146>
18. Doherty P, Gavin KG (2013) Pile aging in cohesive soils. *J Geotech Geoenviron Eng* 139: 1620–1624. [https://doi.org/10.1061/\(ASCE\)GT.1943-5606.0000884](https://doi.org/10.1061/(ASCE)GT.1943-5606.0000884)
19. McCabe BA, Sexton BG, Lehane BM (2013) Operational coefficient of consolidation around a pile group in clay/silt. *Geotech Geol Eng* 31: 183–197. <https://doi.org/10.1007/s10706-012-9579-1>
20. Lehane BM, Phillips DT, Paul TS, et al. (1999) Instrumented piles subjected to combined vertical and lateral loads. *Proceedings of the 12<sup>th</sup> European Conference on Soil Mechanics and Geotechnical Engineering*, Amsterdam, 2: 1145–1150.
21. Phillips DT (2002) Field tests on single piles subjected to lateral and combined axial and lateral loads. PhD Thesis, Trinity College Dublin.
22. Lehane BM (2003) Vertically loaded shallow foundation on soft clayey silt: A case history. *Geotech Eng* 156: 17–26. <https://doi.org/10.1680/geng.2003.156.1.17>
23. Timoney MJ (2015) Strength verification methods for stabilised soil-cement columns: a laboratory investigation of the PORT and PIRT. PhD thesis, University of Galway.



24. Timoney MJ, McCabe BA (2017) Strength verification of stabilised soil-cement columns: a laboratory investigation of the Push-In Resistance Test (PIRT). *Can Geotech J* 54: 789–805. <https://doi.org/10.1139/cgj-2016-0230>
25. Bowen DQ, Rose J, McCabe AM, et al. (1986) Correlation of Quaternary glaciations in England, Ireland, Scotland and Wales. *Quat Sci Rev* 5: 299–340. [https://doi.org/10.1016/0277-3791\(86\)90194-0](https://doi.org/10.1016/0277-3791(86)90194-0)
26. Wilson HE (1972) Recent Geology of Northern Ireland, HMSO, Belfast.
27. Manning PI, Robbie JA, Wilson HE (1970) Geology of Belfast and the Lagan Valley, HMSO, Belfast.
28. Hight DW, Bond AJ, Legge JD (1992) Characterization of the Bothkennar clay: an overview. *Géotechnique* 42: 303–347. <https://doi.org/10.1680/geot.1992.42.2.303>
29. Mitchell JK (1976) *Fundamentals of Soil Behaviour*, 1st edition, London: Wiley.
30. Lutenecker AJ, Cerato A (2001) Surface area and engineering properties of fine-grained soils. *Proceedings of the 15<sup>th</sup> International Conference on Soil Mechanics and Geotechnical Engineering*, 1–3: 603–606.
31. Xu S, Feng Q, Deng Y, et al. (2024) Effect of diatom inclusion on physical property identification of soft clay. *J Soils Sediments* 24: 603–614. <https://doi.org/10.1007/s11368-023-03673-x>
32. Gundersen AS, Hansen RC, Lunne T, et al. (2019) Characterization and engineering properties of the NGTS Onsøy soft clay site. *AIMS Geosci* 5: 665–703. <https://doi.org/10.3934/geosci.2019.3.665>
33. Shibuya S, Tamrakar SB, Thermost N (2001) Geotechnical site characterization on engineering properties of Bangkok Clay. *J Southeast Asian Geotech Soc* 32: 139–151.
34. Low HE, Landon Maynard M, Randolph MF, et al. (2011) Geotechnical characterisation and engineering properties of Burswood clay. *Géotechnique* 61: 575–591. <https://doi.org/10.1680/geot.9.P.035>
35. Zhang X, Liu X, Xu Y, et al. (2024) Compressibility, permeability and microstructure of fine-grained soils containing diatom microfossils. *Géotechnique* 74: 661–675. <https://doi.org/10.1680/jgeot.22.00155>
36. Robertson PK (1990) Soil classification using the cone penetration test. *Can Geotech J* 27: 151–158. <https://doi.org/10.1139/t90-014>
37. Suzuki Y, Lehane BM (2014) Field observations of CPT penetration rate effects in Burswood clay. *Proceedings of 3<sup>rd</sup> International Conference on Cone Penetration Testing*, 403–410.
38. Long M, Colreavy C, Ward D, et al. (2014) Piezoball tests in soft Irish clays. *Proceedings of the 3<sup>rd</sup> International Symposium on Cone Penetration Testing*, Las Vegas, Nevada, 467–475.
39. Houlsby GT, Teh CI (1988) Analysis of the Piezocone in Clay. Conference on Penetration Testing, Balkema, Rotterdam, 777–783.
40. Leroueil S, Lerat P, Hight DW, et al. (1992) Hydraulic Conductivity of a Recent Estuarine Silty Clay at Bothkennar, Scotland. *Géotechnique* 42: 275–288. <https://doi.org/10.1680/geot.1992.42.2.275>
41. Shiwakoti DR, Tanaka H, Tanaka M, et al. (2002) Influences of diatom microfossils on engineering properties of soils. *Soils Found* 42: 1–17. [https://doi.org/10.3208/sandf.42.3\\_1](https://doi.org/10.3208/sandf.42.3_1)

42. McCabe BA, Sheil BB, Buggy F, et al. (2014) Empirical correlations for the compression index of Irish soft soils. *Proc Inst Civ Eng Geotech Eng* 167: 510–517. <https://doi.org/10.1680/geng.13.00116>
43. Burland JB, Eng F (1990) On the Compressibility and Shear Strength of Natural Clays. *Géotechnique* 40: 329–378. <https://doi.org/10.1680/geot.1990.40.3.329>
44. Mesri G, Godlewski PM (1977) Time and stress-compressibility inter-relationship. *J Geotech Eng Div* 103: 417–430. <https://doi.org/10.1061/AJGEB6.0000421>
45. Glossop NH, Saville DR, Moore JS, et al. (1979) Geotechnical aspects of shallow tunnel construction in Belfast estuarine deposits. *Tunnelling* 79, London, 45–56.
46. DeGroot DJ, Landon ME, Poirier SE (2019) Geology and engineering properties of sensitive Boston Blue Clay at Newbury, Massachusetts. *AIMS Geosci* 5: 412–447. <https://doi.org/10.3934/geosci.2019.3.412>
47. Chen C, Wang Y, Sun Z, et al. (2024) Rate effects of cylindrical cavity expansion in fine grained soil. *J Rock Mech Geotech Eng*, in press. <https://doi.org/10.1016/j.jrmge.2024.09.032>
48. Davies JA, Humpheson C (1981) Comparison between the performance of two types of vertical drain beneath a trial embankment in Belfast. *Géotechnique* 31: 19–31. <https://doi.org/10.1680/geot.1981.31.1.19>
49. Jaky J (1944) The coefficient of earth pressure at rest. *J Soc Hung Archit Eng*, 355–358.
50. Ladd CC, Foott R, Ishihara K, et al. (1977) Stress-Deformation and Strength Characteristics. *Proceedings of the 9th International Conference on Soil Mechanics and Foundation Engineering*, Tokyo, 2: 421–494.
51. Padfield CJ, Mair RJ (1983) Design of retaining walls embedded in soft clay, CIRIA report 104.
52. Jardine RJ, Chow FC, Matsumoto T, et al. (1998) A new design procedure for driven piles and its applications to two Japanese clays. *Soils Found* 38: 207–219. <https://doi.org/10.3208/sandf.38.207>
53. Lupini JF, Skinner AE, Vaughan PR (1981) Drained residual strength of cohesive soils. *Géotechnique* 31: 181–213. <https://doi.org/10.1680/geot.1981.31.2.181>
54. Strick van Linschoten CJ (2004) Driven pile capacity in organic clays with particular reference to square piles in Belfast sleetch. MSc thesis, Imperial College London.
55. Doherty P, Gavin KG (2009) Experimental investigation of the effect of shearing rate on the capacity of piles in soft silt. *Contemp Top Deep Found*, 575–582. [https://doi.org/10.1061/41021\(335\)72](https://doi.org/10.1061/41021(335)72)

## Supplementary Information A

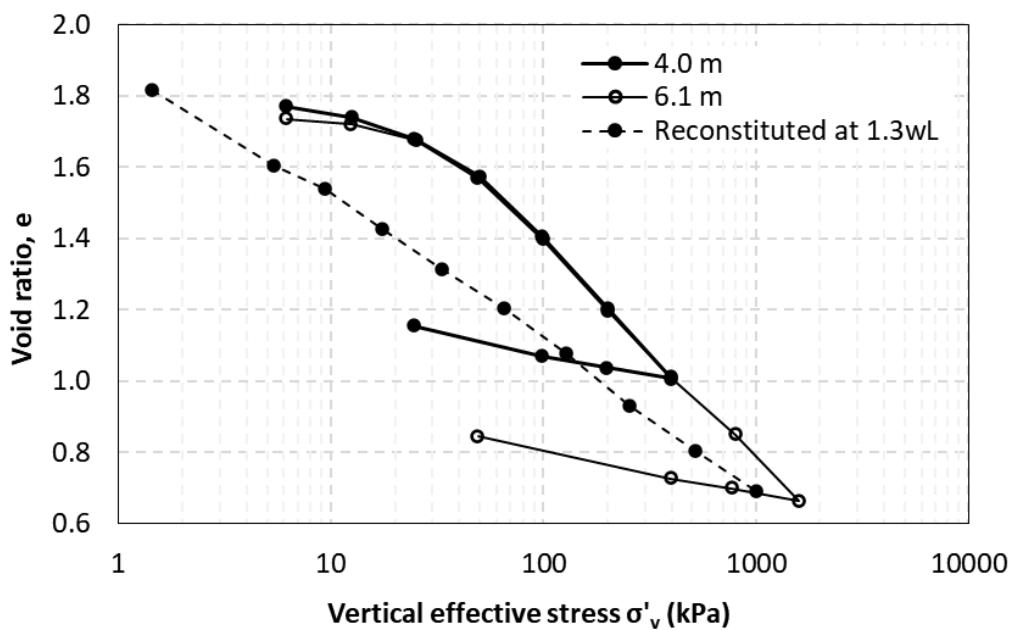
Geotechnical parameters for Stratum 3 sleetch ( $z = 5.5$  m,  $\sigma'_v = 50$  kPa)

Parameter at $\sigma'_v = 50$ kPa	Value
Clay content (%)	28
Fines content (%)	96
Organic content (%)	11
Bulk unit weight ( $\text{kN/m}^3$ )	15.8
Plasticity index $I_p$ (%)	38.5

Liquidity index $I_L$ (-)	0.75
Corrected cone tip resistance $q_t$ (kPa)	310
Normalised undrained shear strength from <i>in situ</i> vane $s_{uvane}/\sigma'_{v0}$ (with Bjerrum correction for plasticity index applied) (-)	0.4
Shear wave velocity $V_s$ (m/s)	73
Limit pressure $p_{lim}$ (kPa)	151
Vertical permeability $k_{v0}$ (m/s)	$1.5 \times 10^{-10}$
Coefficient of consolidation (vertical) $c_v$ (m <sup>2</sup> /year)	2.8
Coefficient of consolidation (horizontal) $c_h$ (m <sup>2</sup> /year)	7–12
Preconsolidation pressure $\sigma'_{vy}$ (kPa)	55
Compression index $C_c$ (-)	0.67
Creep coefficient $C_\alpha$ (-)	0.0124
Constant volume friction angle ( $^\circ$ )	33.5

## Supplementary Information B

Example  $e$ - $\log \sigma'_v$  plots



AIMS Press

© 2025 the Author(s), licensee AIMS Press. This is an open access article distributed under the terms of the Creative Commons Attribution License (<https://creativecommons.org/licenses/by/4.0>)